-80-3623

CONF-810310--1

MASTER

TITLE: METHODS FOR DECONVOLVING SPARSE POSITIVE DELTA FUNCTION SERIES

AUTHOR(S): H. J. Trussell and L. A. Schwalbe

SUBMITTED TO: 1981 IEEE International Conference on Acoustics, Speech and Signal Processing, March 30-April 1, 1981, Atlanta, GA.

DISCLAIMER

University of California

LOS ALAMOS SCIENTIFIC LABORATORY
Post Office Box 1663 Los Alamos, New Mexico 87545
An Affirmative Action/Equal Opportunity Employer

Form No. 836 R3
St. No. 2629
12/78

UNITED STATES
DEPARTMENT OF ENERGY
CONTRACT W-7405-ENG. 36

METHODS FOR DECONVOLVING SPARSE POSITIVE DELTA FUNCTION SERIES*

H. J. Trussell
North Carolina State University
Raleigh, North Carolina

L. A. Schwalbe
University of California Los Alamos Scientific Laboratory
Los Alamos, New Mexico

ABSTRACT

Sparse delta function series occur as data in many chemical analysis and seismic methods. This original data is often sufficiently degraded by the recording instrument response that the individual delta function peaks are difficult to distinguish and measure. A method, which has been used to measure these peaks, is to fit a parameterized model by a nonlinear least squares fitting algorithm. The deconvolution approaches described here have the advantage of not requiring a parameterized point spread function, nor do they expect a fixed number of peaks.

Two new methods will be presented. The maximum power technique will be reviewed. A maximum a posteriori technique will be introduced. Results on both simulated and real data by the two methods will be presented. The characteristics of the data can determine which method gives superior results.

INTRODUCTION

There are two main requirements for the definition of a signal restoration method. The first is the data formation model. The second, and more controversial requirement, is the restoration criterion. It is in deciding upon this criterion that the operator has the most latitude in determining the appearance of the restored signal. Because of this great latitude this is the step most frequently subjected to criticism.

The choice of the data formation model is a factor of many things besides realistic accuracy. Some of these other factors are mathematical tractability, computational difficulty, and subjective results. One model we will use is the standard linear model. This can be written in matrix/vector notation as

$$\underset{\sim}{g} = \underset{\sim}{H}\underset{\sim}{f} + \underset{\sim}{n} , \qquad (1)$$

where $\underset{\sim}{g}$ is an n x 1 data vector,

$\underset{\sim}{H}$ is an n x n point spread function matrix,

$\underset{\sim}{f}$ is an n x 1 vector of the original signal,

$\underset{\sim}{n}$ is an n x 1 vector of random noise.

While not always the most accurate, this model has proved useful in many applications. In particular it has proved adequate for one of the algorithms described here.

*Work performed under the auspices of the U.S. Dept. of Energy, Contract No. W7405-ENG-36.

A modification of the above model is useful for Poisson noise. This model is more accurate when the sensor is a photon-counting device as are many x-ray detectors. Here we write

$$\underset{\sim}{g} = n(\underset{\sim}{H}\underset{\sim}{f}) , \qquad (2)$$

where g(i) is obtained by a Poisson noise process $\underset{\sim}{n}(\cdot)$ with a mean of the i^{th} element of $\underset{\sim}{H}\underset{\sim}{f}$.

Once the model is selected, although sometimes before, a restoration criterion can be defined. It is in this definition that the peculiar characteristics of the signal can be taken into account. The signals that are being considered here are sparse positive delta function trains. A signal of a few positive spikes can arise in many areas including chemical analysis and seismology. The data we will use comes from x-ray fluorescence spectra. In this process a sample material is irradiated by an x-ray source; the material then fluoresces at discrete energies characteristic of the component elements. The intensity of detected radiation at each energy is required to determine the amount of the element present.

This ideal data is degraded by blurring and noise. The blur is caused by the imperfect response of the recording instrument. The energy of every detected photon is not measured correctly. The noise arises from the statistical nature of the emission of photons from the sample and the limited efficiency of the detector.

Because of the nature of this type of signal, the usual restoration criteria do not produce good results. We would like to recreate the original peaks or at least separate the peaks so that the integrated area under each one can be easily measured. Our interest in the peak values at the expense of the background values precludes the use of the minimum mean square error (or Wiener) filter. Likewise, constrained least squares deconvolution, which finds the smoothest solution satisfying a residual constraint, would not be appropriate for this application. Linear filters, in general, do not seem to produce acceptable results for this special case. Let us now consider two methods designed with this type of data in mind.

MAXIMUM POWER

The ideal signal, which was degraded to give our data, consisted of a series of spikes on a relatively constant background. The restoration criterion that is selected must not only allow but also encourage such spikes to exist. Furthermore, the criterion must result in a restored signal, which could have reasonably given rise to the data.

From the examination of the constrained least squares method and later maximum a posteriori methods, minimizing a quadratic function of the estimate, $\hat{f}$ results in a "smooth" restoration. The result that is desired here is just the opposite. Thus, a simple criterion is to maximize the function $f^T f$. It is noted that this function is unbounded unless some constraint is placed on the solution.

The solution that is found must be feasible, that is, it must be plausible that the solution could have been degraded by the chosen model to have produced the given data. One way to test this is to examine the residual of the linear model

$$r = g - H\hat{f} \quad . \tag{3}$$

If $\hat{f} = f$, the true solution, then $r = n$ the noise. Since we can never know what the true noise is, the best we can do is to impose a condition that r is like noise. While the desired statistical properties of r can be easily defined, finding methods of enforcing these properties upon the residual is more difficult. A less demanding statistical constraint is used in practice. In this paper, a feasible solution is one that satisfies

$$\|g - H\hat{f}\|^2 = \|n\|^2 \pm \varepsilon \quad , \tag{4}$$

where ε is arbitrary. This equation says that the variance of the residual is close to the variance of the noise. It is noted that this constraint does not explicitly require f to be nonnegative. A special step in the algorithm is required to enforce this restriction.

The maximum power solution is the estimate $\hat{f}$, which satisfies Eq. (4) and has the largest norm $\|\hat{f}\|$. The method for obtaining this solution is a double iteration method described in [1]. First, a feasible solution is found by an iterative method, then it is moved in the direction of maximum power (norm). Another feasible solution is found from this starting point as the cycle starts again.

Maximum power restoration is based on the linear model (1). It has been mentioned that this model is not the most accurate for most cases. We will now examine a method based on the more accurate Poisson noise model (2).

MAXIMUM A POSTERIORI/POISSON

An advantage of the maximum a posteriori restoration method is its versatility. This method maximizes the posterior probability density, $p(f|g)$, which by Bayes' law is a function of the prior densities and is written

$$p(f|g) = \frac{p(g|f)p(f)}{p(g)} \quad . \tag{5}$$

The maximization then is the restoration criterion. The solution has been derived for many models and many a priori probability distributions.

The probabilities that need to be defined are $p(g|f)$ and $p(f)$. The former is just the Poisson noise process and is defined by

$$p(g|f) = \prod_{i=1}^{N} \frac{e^{-\bar{g}_i}}{g_i!} \bar{g}_i^{\,g_i} \quad , \tag{6}$$

where $\bar{g}_i$ is the i^{th} element in the vector Hf. Because of the nature of x-ray fluorescence it is reasonable to assume that the ideal signal is also Poisson distributed, hence

$$p(f) = \prod_{i=1}^{N} \frac{e^{-\bar{f}_i} \bar{f}_i^{\,f_i}}{f_i!} \quad , \tag{7}$$

where the overbar denotes the mean.

To derive the solution from Eqs. (5-7) we take the natural logarithm of Eq. (5) and substitute in Eqs. (6) and (7). Stirling's approximation for the factorial is used to obtain the function

$$\Psi(f) = -\sum_{i=1}^{N} \bar{g}_i + \Sigma g_i \ln \bar{g}_i - \Sigma g_i \ln g_i + \Sigma g_i - \Sigma \bar{f}_i + \Sigma f_i \ln \bar{f}_i - \Sigma f_i \ln f_i + \Sigma f_i \quad . \tag{8}$$

Substituting Hf for $\bar{g}$, differentiating with respect to f, and setting the result equal to zero, we obtain the implicit solution

$$\ln f = \ln \bar{f} + \frac{H^T g}{Hf} - H^T 1 \tag{9}$$

or

$$f = \bar{f} \exp H^T \left[\frac{g}{Hf} - 1 \right] , \tag{10}$$

where $1 = (1,1,\ldots,1)^T$, and the division and multiplication of vectors is done pointwise. It should be noted here that the solution to Eq. (10) is implicitly nonnegative.

The solution method is the modified Picard iteration [2], which is given by

$$f_{k+1} = \alpha_k f_k + (1 - \alpha_k)\bar{f} \exp\left[H^T \left(\frac{g}{Hf_k} - 1 \right) \right] . \tag{11}$$

where [illegible]$_k$ is a convergence acceleration term. The a priori average $\bar{f}$ can be fixed at the start of the iteration or it can vary at each iteration. It has been found that letting $\bar{f} = f_k$ produces the best results. This is reasonable if the mean is the solution to which we wish the algorithm to converge. The estimate of the mean should improve with successive iterations.

The two methods just described are based on different models and have very different appearing solution equations. The two iterative algorithms have one factor in common: the solution at the $(k + 1)^{th}$ step is the solution at the k^{th} step plus a multiple of that solution. This characteristic means that high values will be emphasized and low values deemphasized. This is the kind of behavior that is desired for the type of functions discussed in this paper.

RESULTS

The restoration methods were compared on four computer simulations and on one set of actual x-ray fluorescence data. The parameters that were varied in the simulations were the noise level and the background intensity. The magnitudes of the spikes in the simulated data were chosen to be realistically similar to the actual data. The results of the applications of these methods are seen in the figures. Because the range of the data is large compared to the magnitude of some of the effects that are important, the results are plotted on two scales.

In the case of a low noise level and zero background (Fig. 1) the maximum power gives the correct peak values within 1% accuracy. The MAP/Poisson method gives an integrated value about the peaks of the same accuracy, however, the restored peaks are not as well defined. There are more obvious noise artifacts along the baseline of the maximum power restoration. These spike artifacts are caused by the algorithm generating a maximum power solution in a region of the data where it is inappropriate.

The integrated value of the highest peak of the MAP/Poisson method for the case of low background and high noise (Fig. 2) is again within 1% of the correct value. The integrated value of the same peak for the maximum power restoration is over 2% high. This again reflects the nature of maximum power; adding noise is adding power to the total signal. The price of the good separation appears to be numerical accuracy.

The other two cases clearly show the problem that a high background gives the maximum power method (Figs. 3 and 4). The case of high noise and high background (Fig. 4) causes artifacts of such magnitude in the maximum power solution that the smallest peak is difficult to detect. The MAP/Poisson method produces a distinct undershoot about the peaks that is undesirable for the cases of high background.

The restoration of actual recorded (Fig. 5) shows the same properties as the simulations. This case falls somewhere between the high and low noise cases and combines high background on one side of the peaks and low on the other. The separation of the peaks is better in the maximum power restoration. The integrated peak values can still be reliably estimated from the MAP/Poisson solution. Both methods yield integrated values that are within 5% of the known values for this experiment.

CONCLUSIONS

Both methods produce results that are superior to the usual linear restoration methods for the sparse delta function series signal. The maximum power method appears to be of more limited value than the MAP/Poisson method. This is a result of its global definition; that is, it produces a maximum power restoration in areas of little signal power where this criterion is inappropriate. This characteristic could be altered by local processing of the signal.

The MAP/Poisson method is less aggressive than maximum power and is less sensitive to noise. Although the separation of peaks is less definite, the numerical accuracy is greater in the case of higher noise levels. Because of this the MAP method is probably the more useful method in the general case.

Future work on the maximum power method might concentrate on an automatic method of detecting when to apply that algorithm. Methods of eliminating the effects of high backgrounds also need study. The undershoot beside peaks in the MAP/Poisson scheme needs to be corrected. It would be interesting to see if the methods could be combined to give the good separation of one and the stability of the other.

REFERENCES

[1] H. J. Trussell, "Maximum power restoration," to be published IEEE ASSP.

[2] Isaacson and H. B. Keller, Analysis of Numerical Methods, John Wiley & Sons, New York, 1966, pp 120-123.

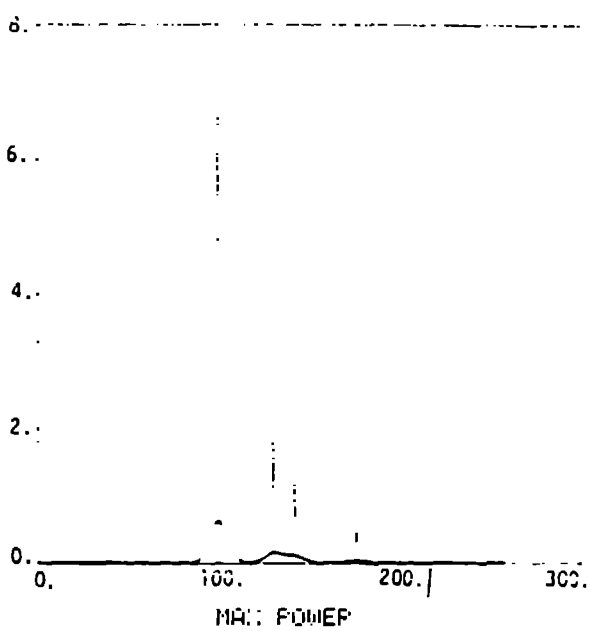

Fig. 1a. Maximum power restoration/low noise, low background.

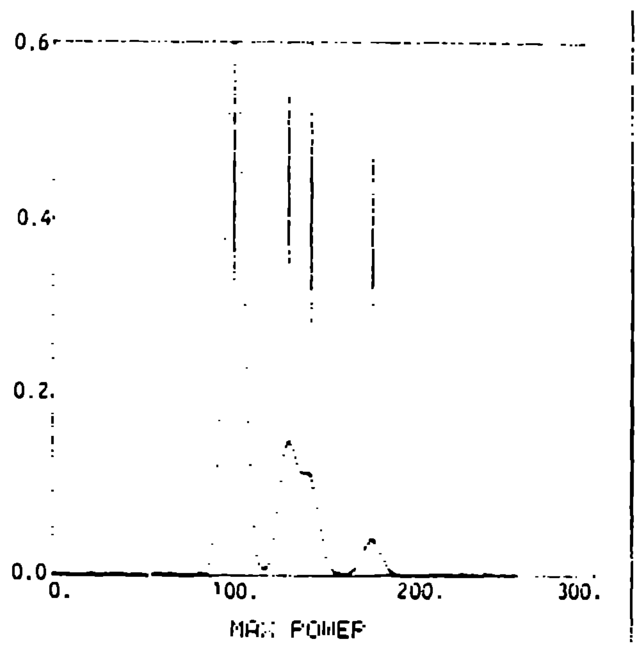

Fig. 1b. Maximum power restoration/low noise, low background.

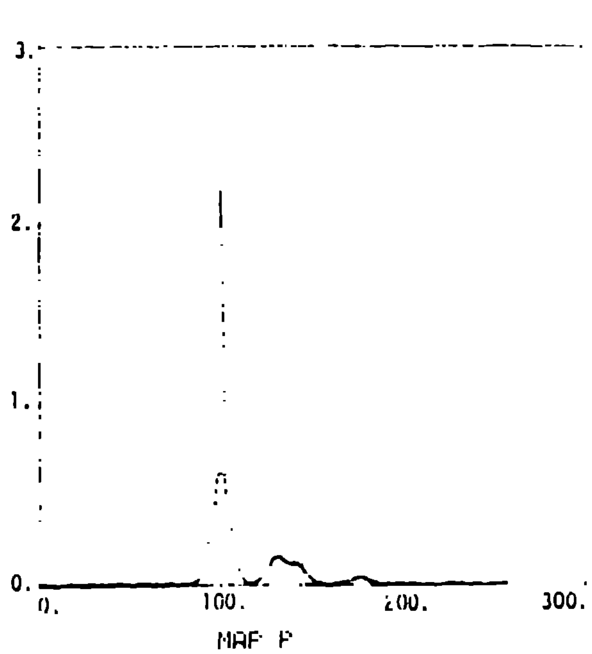

Fig. 1c. MAP/Poisson restoration/low noise, low background.

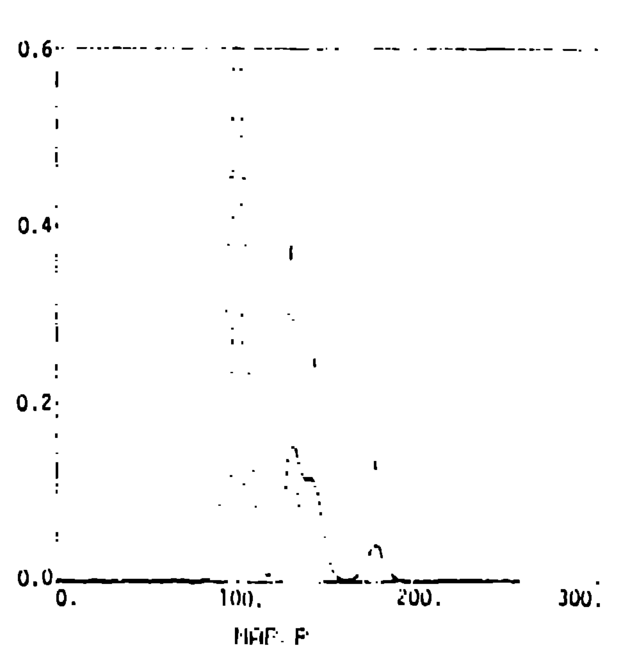

Fig. 1d. MAP/Poisson restoration/low noise, low background.

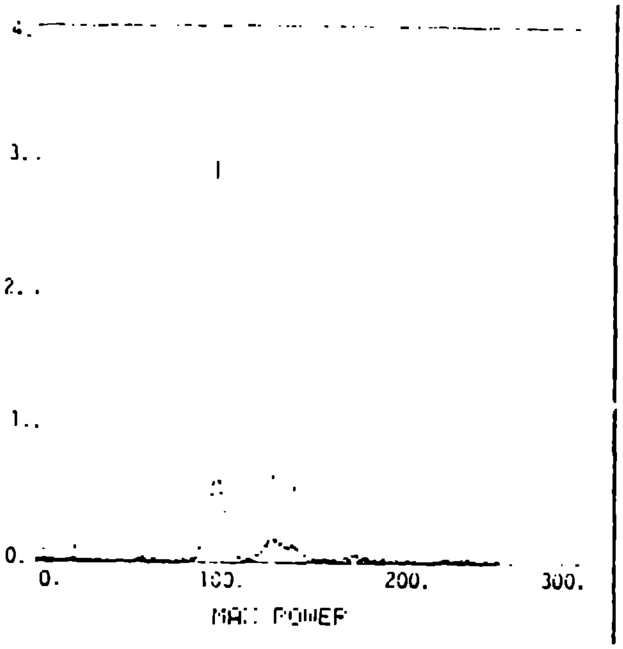

Fig. 2a. Maximum power restoration/high noise, low background.

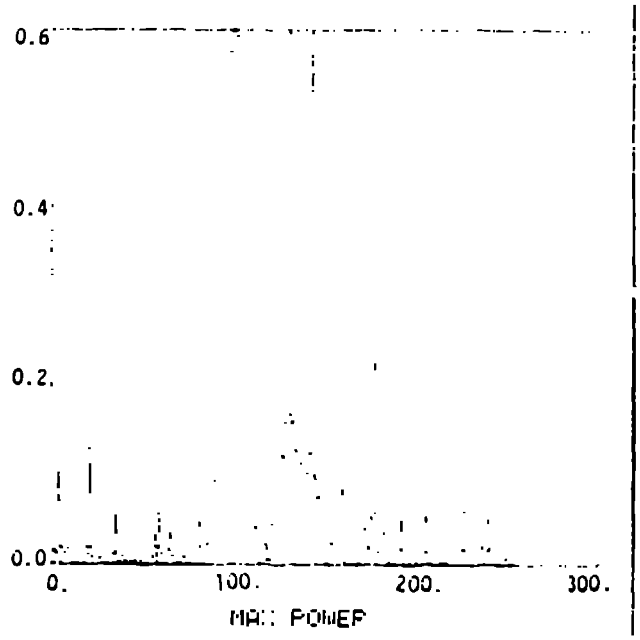

Fig. 2b. Maximum power restoration/high noise, low background.

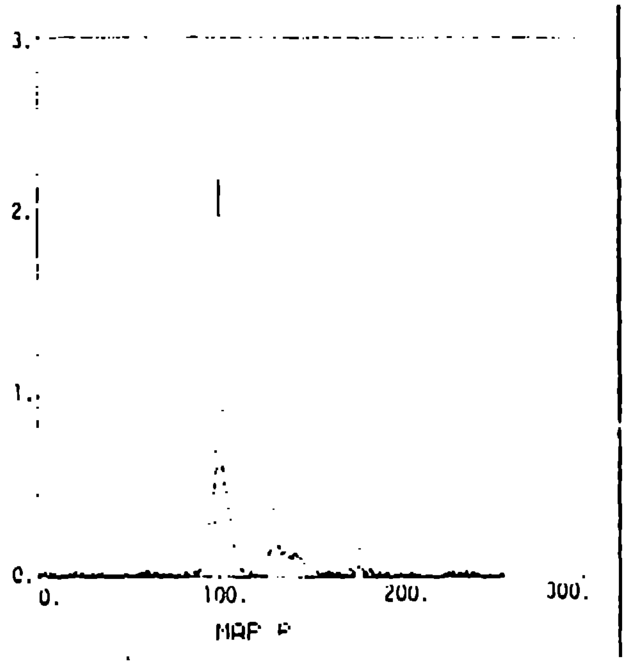

Fig. 2c. MAP/Poisson restoration/high noise, low background.

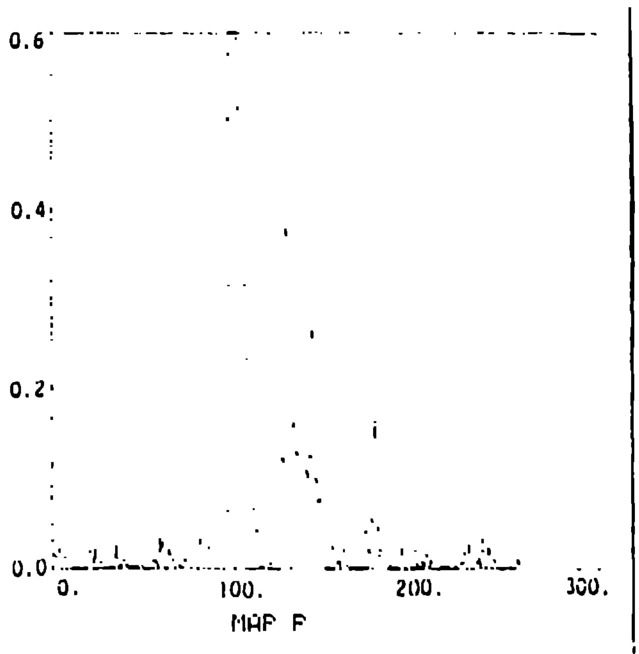

Fig. 2d. MAP/Poisson restoration/high noise, low background.

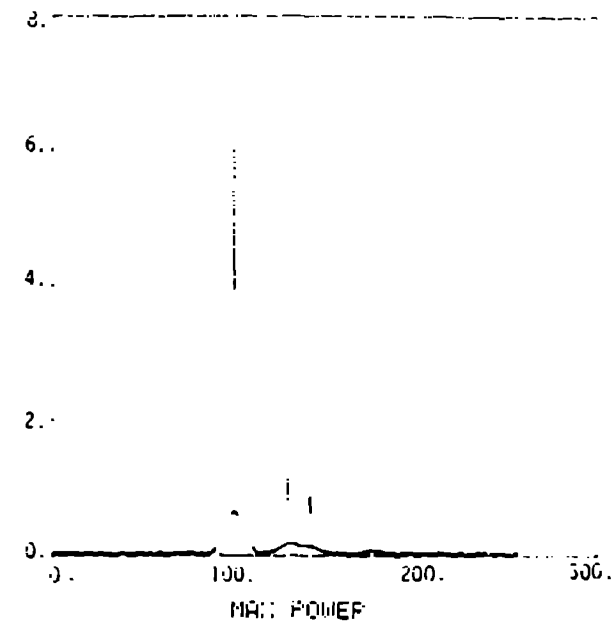

Fig. 3a. Maximum power restoration/low noise, high background.

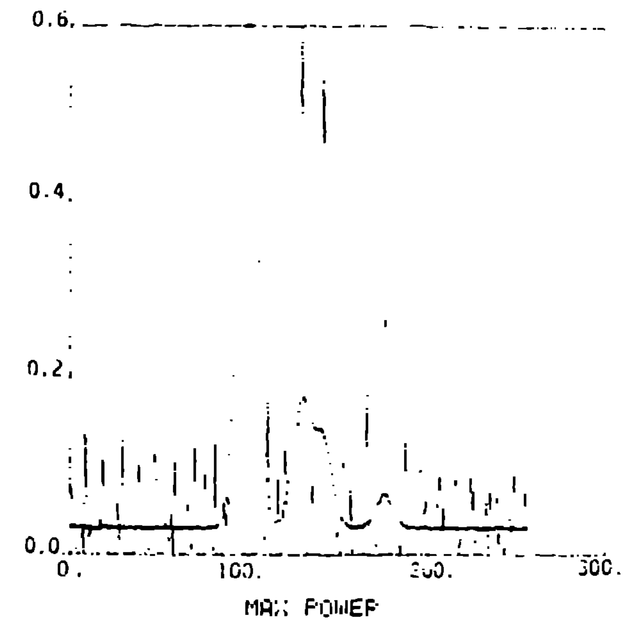

Fig. 3b. Maximum power restoration/low noise, high background.

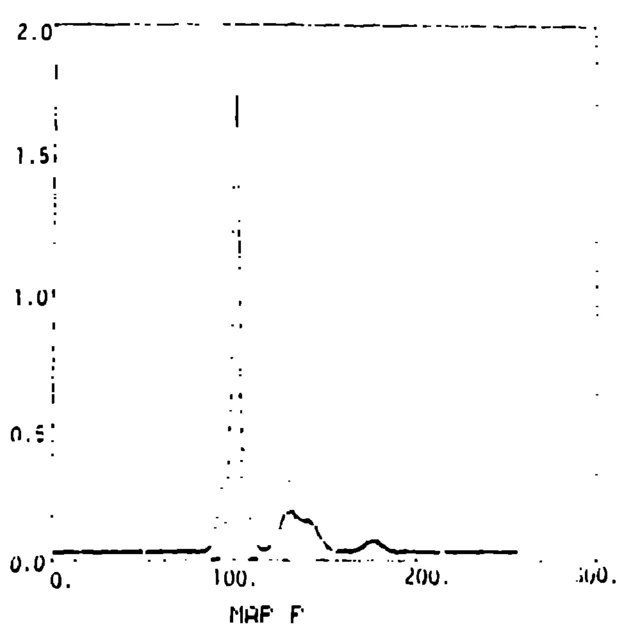

Fig. 3c. MAP/Poisson restoration/low noise, high background.

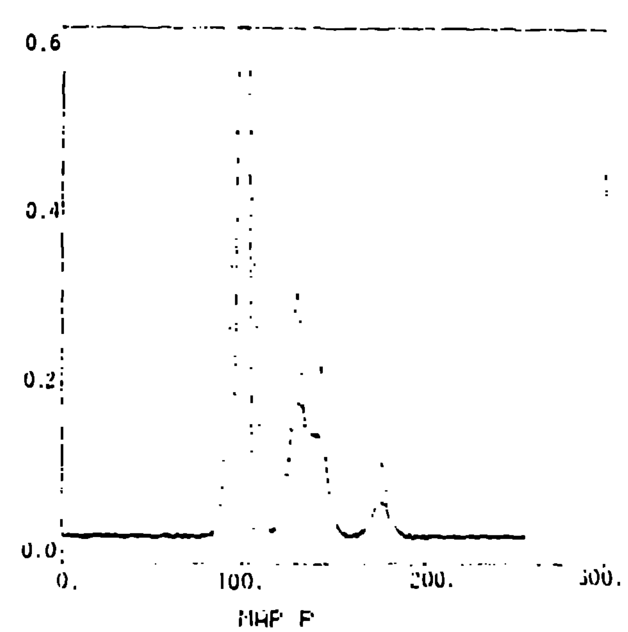

Fig. 3d. MAP/Poisson restoration/low noise, high background.

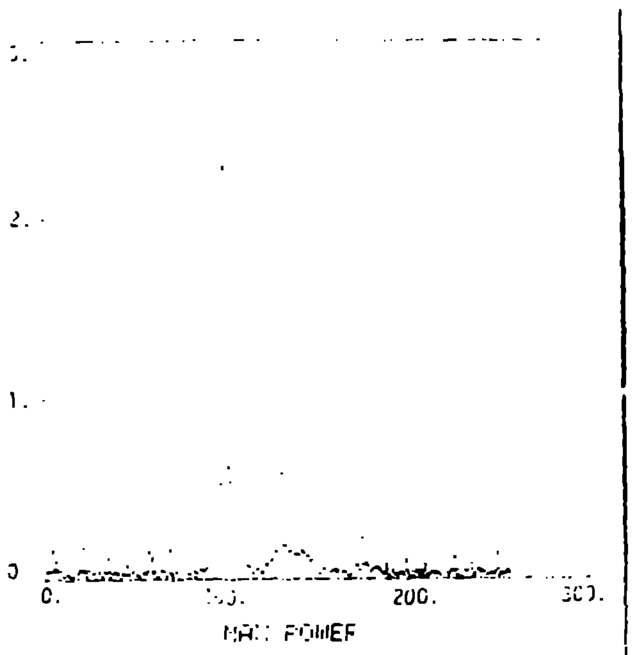

Fig. 4a. Maximum power restoration/high noise, high background.

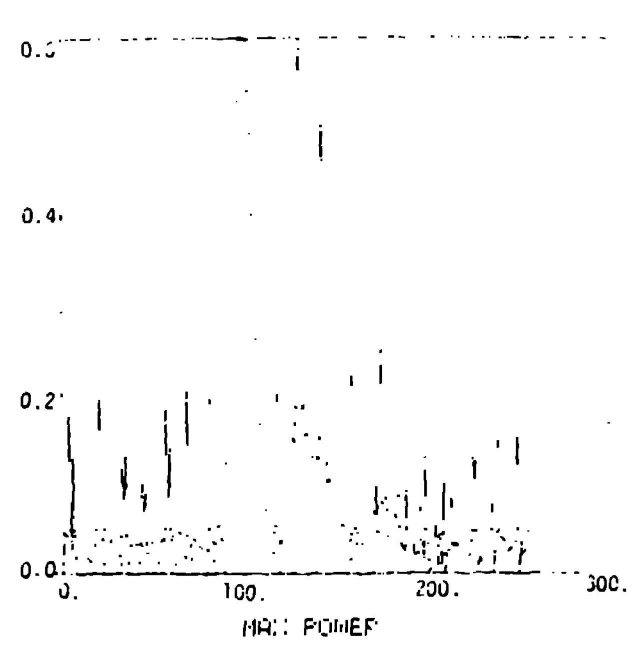

Fig. 4b. Maximum power restoration/high noise, high background.

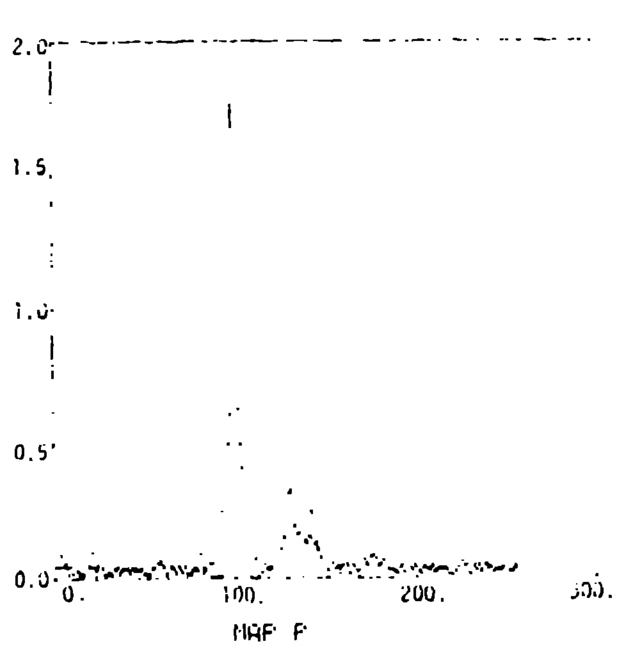

Fig. 4c. MAP/Poisson restoration/high noise, high background.

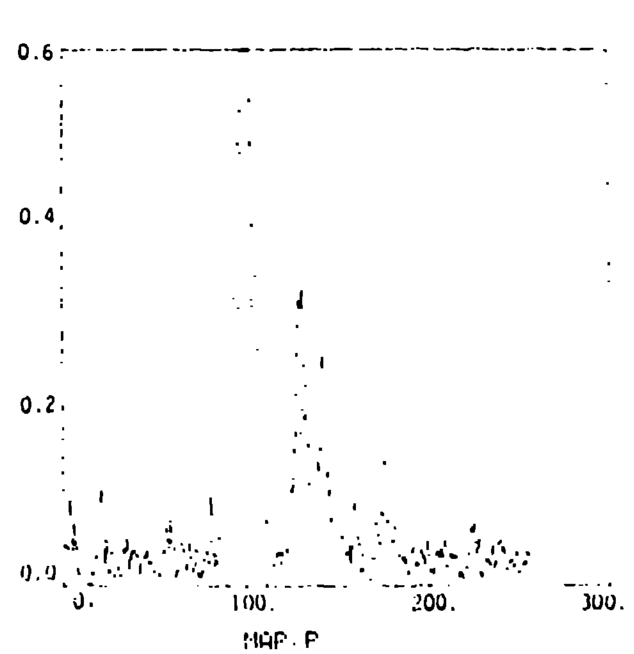

Fig. 4d. MAP/Poisson restoration/high noise, high background.

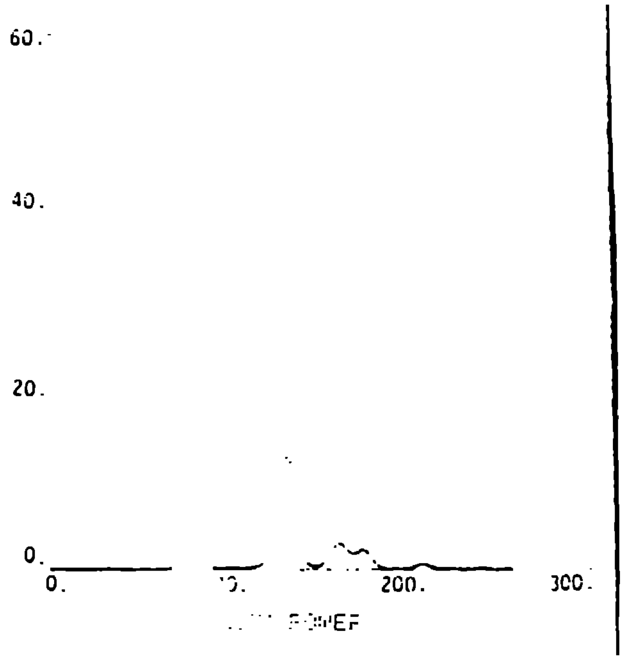

Fig. 5a. Maximum power restoration of original x-ray fluorescence data.

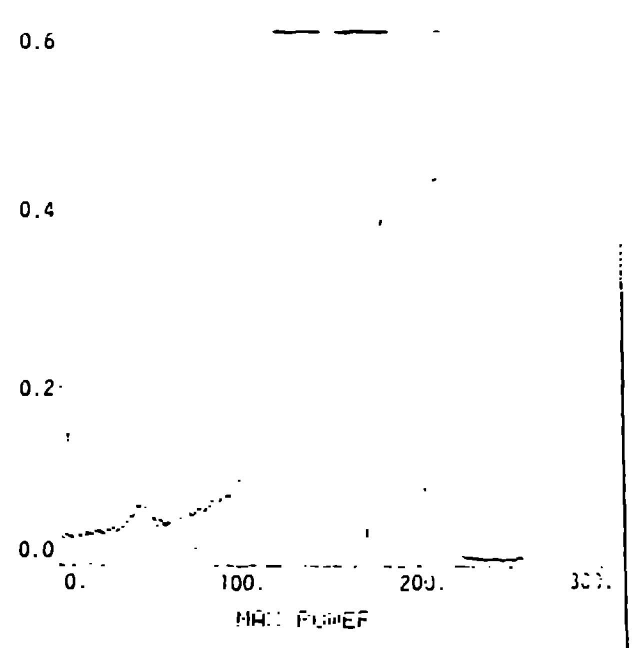

Fig. 5b. Maximum power restoration of original x-ray fluorescence data.

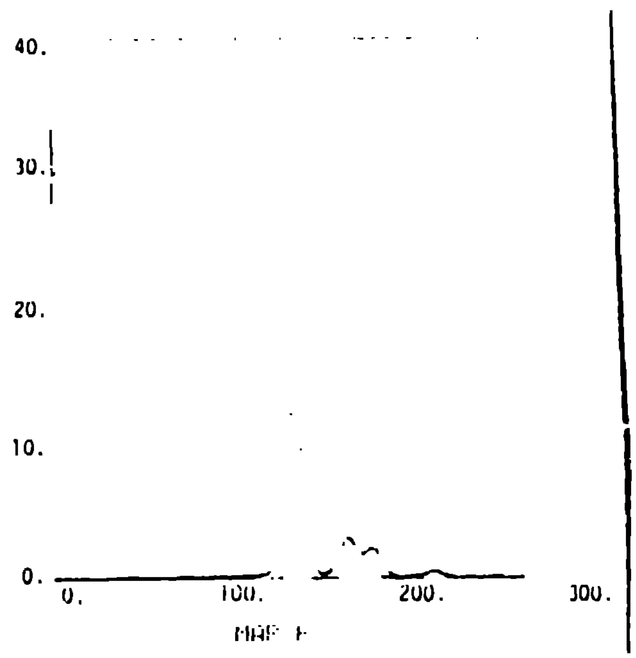

Fig. 5c. MAP/Poisson restoration of original x-ray fluorescence data.

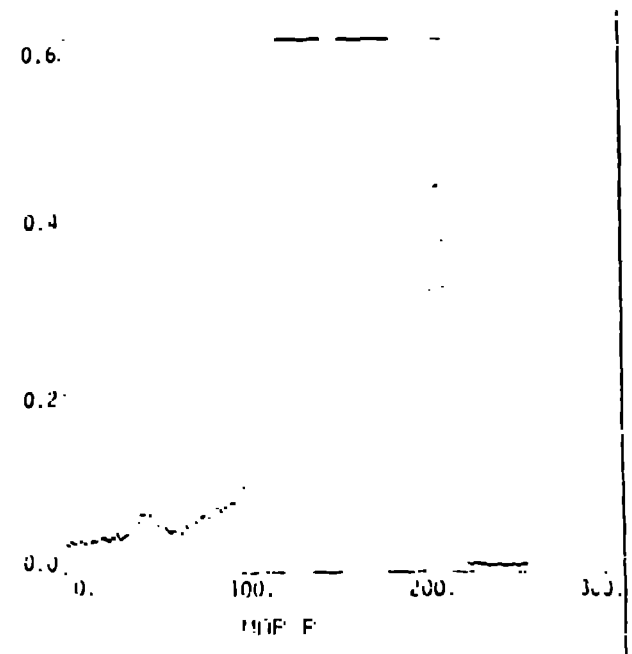

Fig. 5d. MAP/Poisson restoration of original x-ray fluorescence data.